

Supporting Information (SI)

for

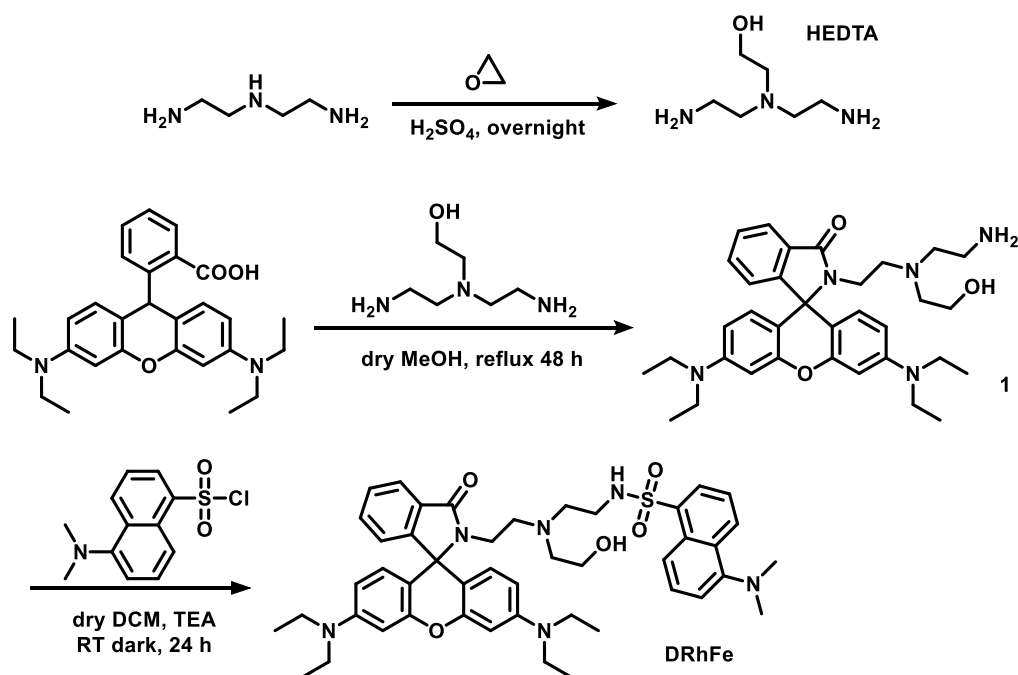
A Reversible FRET Fluorescent Probe for Ratiometric Tracking of Endogenous Fe³⁺ in Ferroptosis

Jing Gao,^{†,‡} Yueqin He,^{§,‡} Yuncong Chen,^{*,†} Dongfan Song,[†] Yuming Zhang,[†] Fen Qi,[†] Zijian Guo,[†] and Weijiang He^{*,†}

Table of Contents

- S1. Synthesis and characterization of compound **DRhFe**
- S2. UV-Vis titration of **DRhFe** by Fe³⁺
- S3. Characterization of Fe³⁺/**DRhFe** complex
- S4. Determination of quantum yield
- S5. Spectroscopic sensing selectivity of **DRhFe** for Fe³⁺
- S6. Spectroscopic response of **DRhFe** to Fe³⁺
- S7. Fluorescent pH-dependence of **DRhFe**
- S8. Cytotoxicity determination of **DRhFe**
- S9. Ratiometric fluorescence imaging for labile Fe³⁺ in HeLa cells
- S10. Ratiometric imaging of endogenous labile Fe³⁺ in cells undergoing ferroptosis
- S11. References

S1. Synthesis and characterization of compound DRhFe



Scheme S1. Synthesis of compound **DRhFe**.

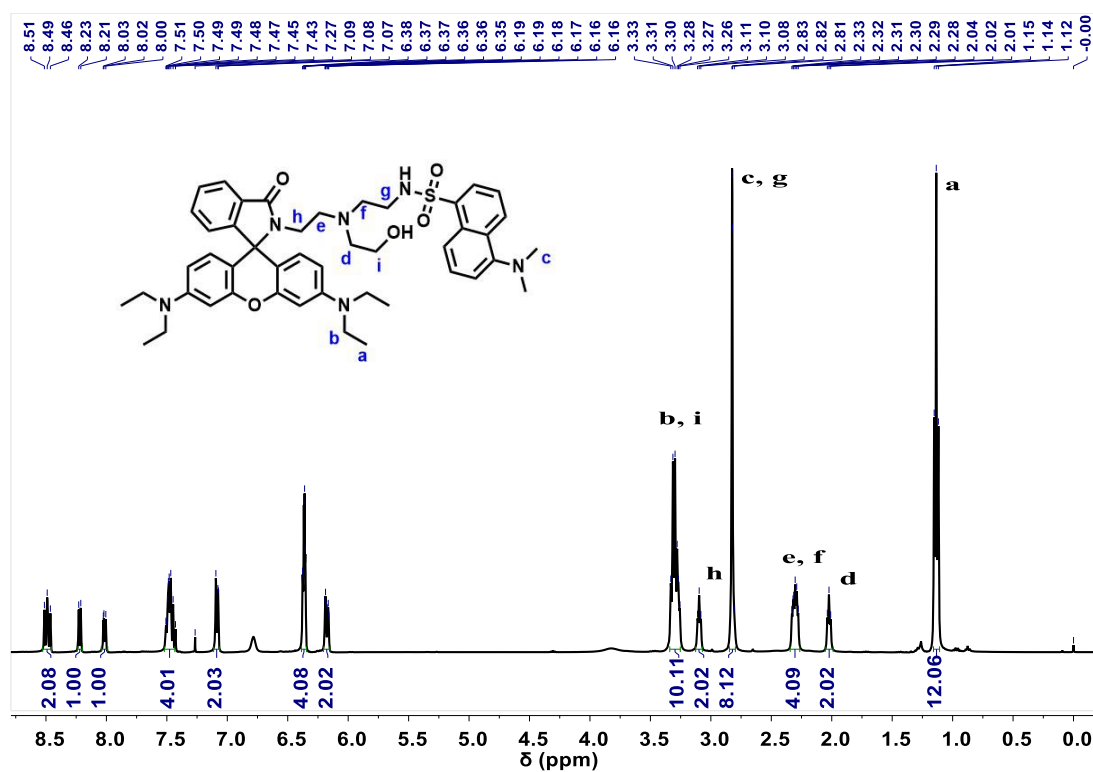


Figure S1 ^1H NMR spectrum of **DRhFe** (400 MHz, CDCl_3).

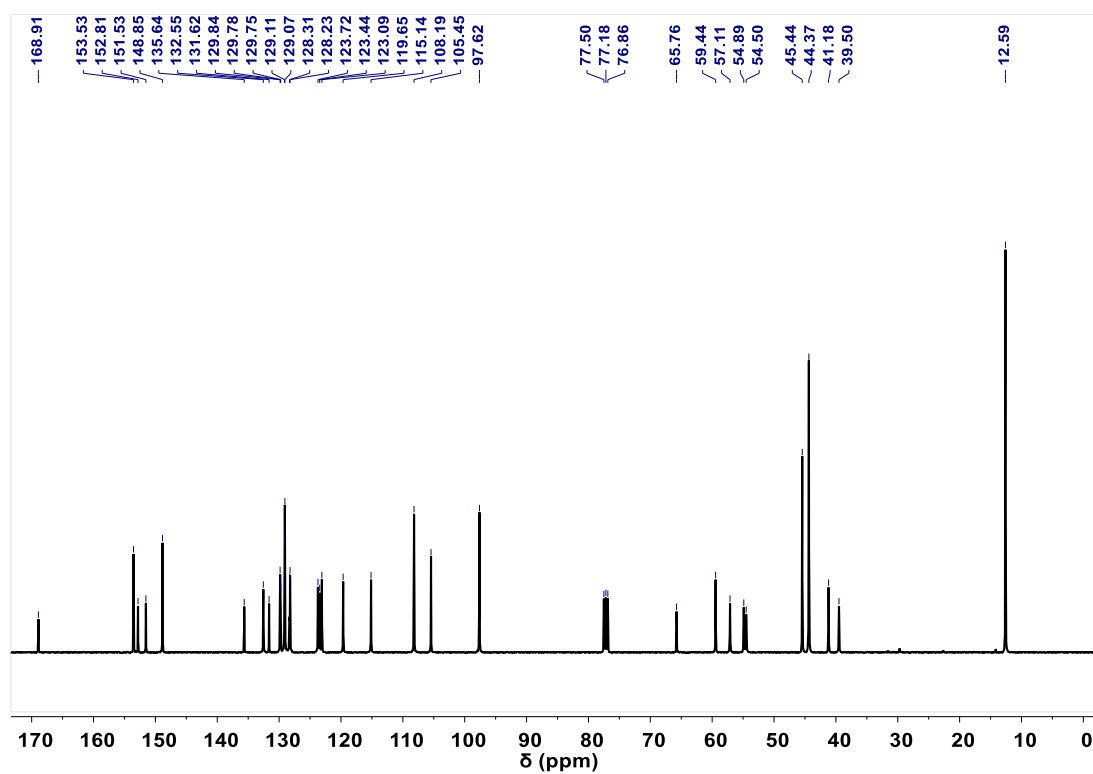


Figure S2 ^{13}C NMR spectrum of **DRhFe** (101 MHz, CDCl_3).

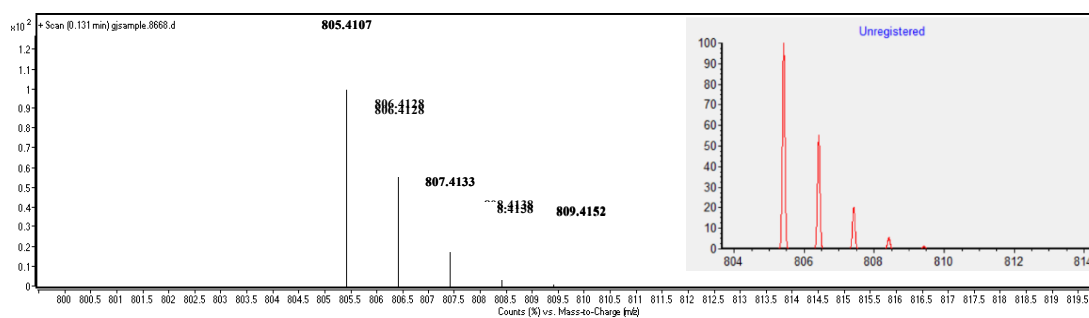


Figure S3 High-resolution mass spectrum of **DRhFe**. The red one is the simulated isotopic distribution pattern of $[\text{DRhFe}+\text{H}]^+$.

S2. UV-Vis titration of DRhFe by Fe³⁺

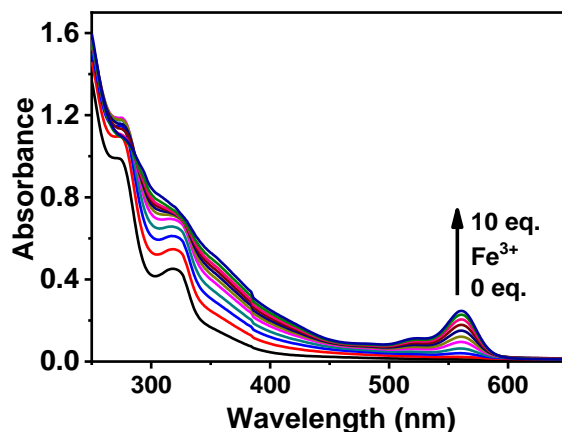


Figure S4 Absorption spectra of 25 μM DRhFe in $\text{H}_2\text{O}/\text{DMSO}$ (99:1, v/v) obtained via titration with Fe^{3+} (0-250 μM).

S3. Characterization of Fe³⁺/DRhFe complex

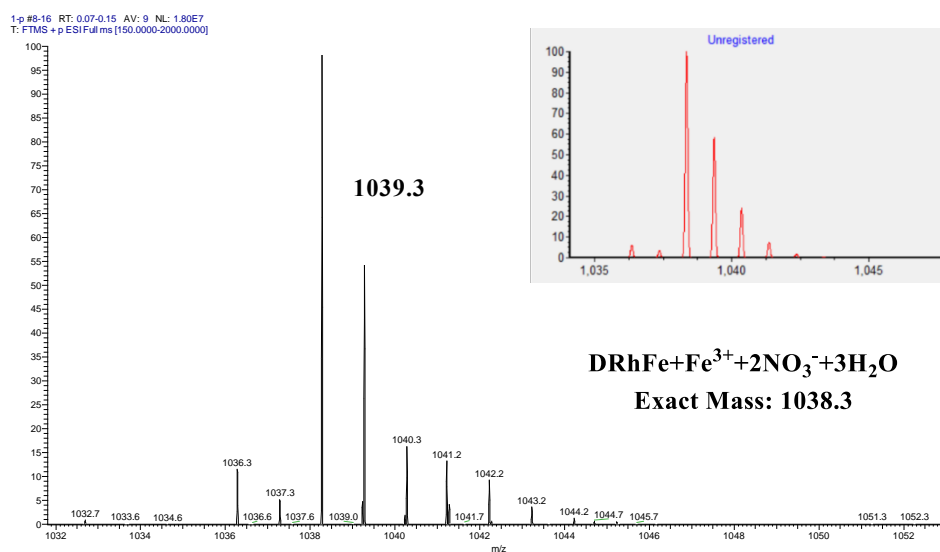


Figure S5 ESI mass spectrum of DRhFe mixed with excessive $\text{Fe}(\text{NO}_3)_3 \cdot 9\text{H}_2\text{O}$ in CH_3CN . The red one is the simulated isotopic distribution pattern of $[\text{DRhFe} + \text{Fe} + 2\text{NO}_3 + 3\text{H}_2\text{O}]^+$.

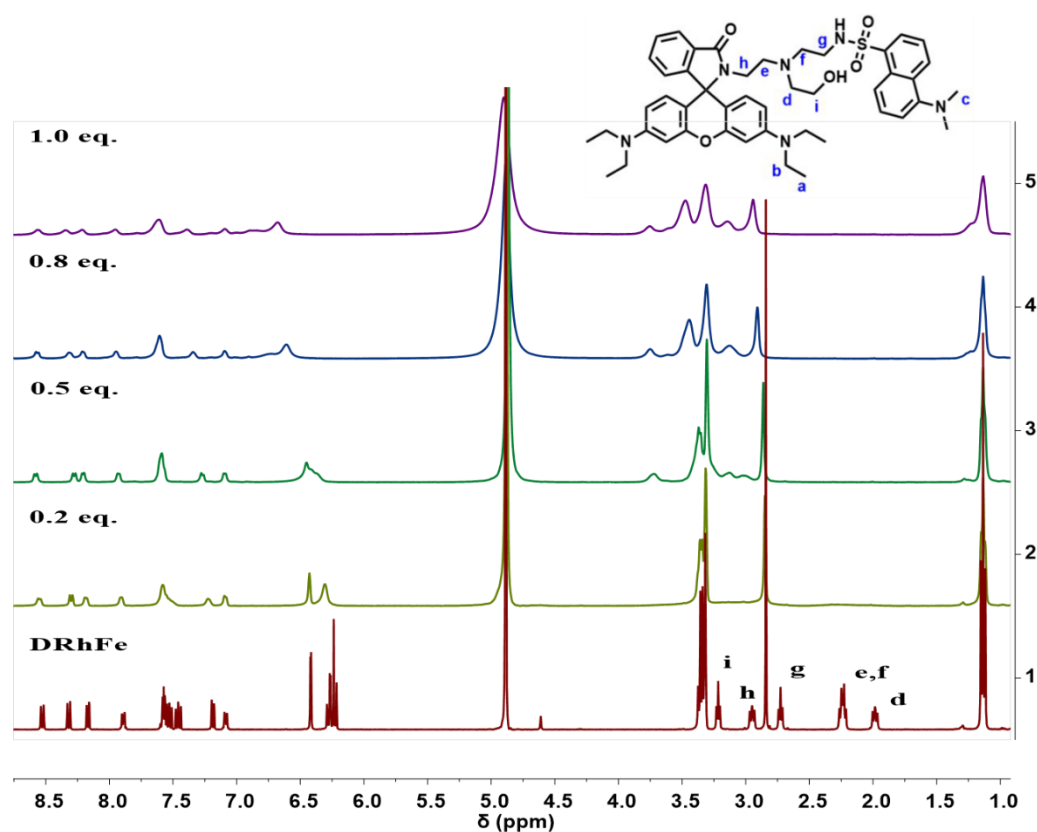


Figure S6 ^1H NMR spectra of **DRhFe** upon titration by $\text{Fe}(\text{NO}_3)_3$ in CD_3OD .

S4. Determination of quantum yield

Fluorescence quantum yield of **DRhFe** and $\text{Fe}^{3+}/\text{DRhFe}$ complex were determined in EtOH using an integrating sphere on Horiba FluoroMax-4 spectrofluorometer, and the absorbance of samples at their respective excitation wavelengths was controlled to be lower than 0.05.

Table S1. Photoluminescence quantum yields of **DRhFe**.

Compounds	Φ_{dns}	Φ_{rho}
10 μM DRhFe	71.31%	-
10 μM DRhFe + 30 eq $\text{Fe}(\text{NO}_3)_3$	-	23.62%

S5. Spectroscopic sensing selectivity of DRhFe for Fe³⁺

Stock solutions of Cd²⁺, Co²⁺, Cu²⁺, Mn²⁺, Ni²⁺, K⁺, Mg²⁺, Ca²⁺, Na⁺, Zn²⁺, Fe²⁺, Al³⁺, Cr³⁺, Hg²⁺, and Fe³⁺ were prepared via dissolving the related salts in the deionized water. The concentration of Al³⁺, Cr³⁺, Mn²⁺, Fe²⁺, Co²⁺, Ni²⁺, Cu²⁺, Zn²⁺, Ag⁺, Cd²⁺, Ba²⁺, Hg²⁺, Pb²⁺, Fe³⁺ is 10 mM and that for K⁺, Ca²⁺, Na⁺, Mg²⁺ is 1 M. For all spectroscopic study, the stock solutions were further diluted to obtain the desired concentrations for spectroscopic determination.

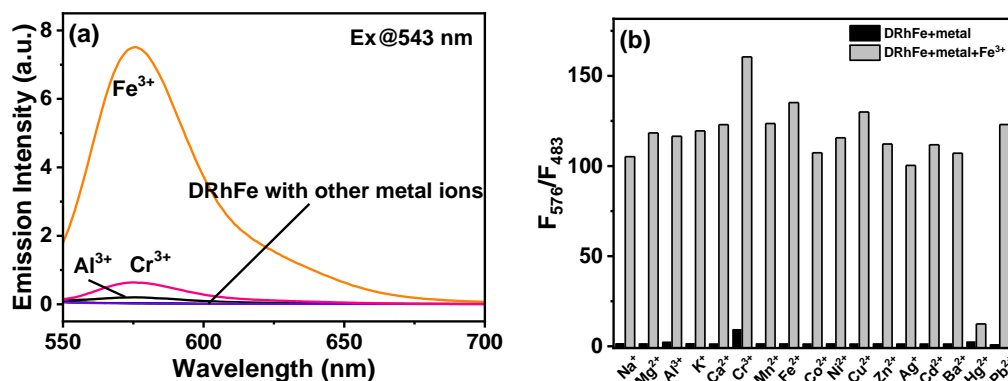


Figure S7 (a) Emission spectra of **DRhFe** (10 μM) obtained in the presence of different metal ions upon excitation at 543 nm. (b) Emission ratio F₅₇₆/F₄₈₃ of **DRhFe** (9.6 μM) obtained in the presence of different metal ions (black) and the Fe³⁺-response in the presence of the marked cations (grey) upon excitation at 405 nm and 543 nm. [Fe³⁺] = 100 μM, [Na⁺, K⁺, Mg²⁺, Ca²⁺] = 1000 μM, and [other metal ions] = 200 μM.

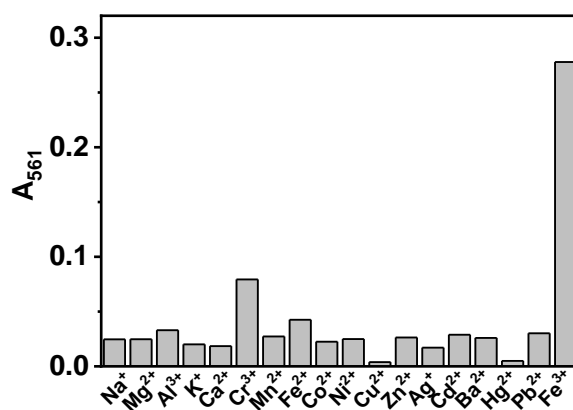


Figure S8. Absorbance changes at 561 nm of **DRhFe** (10 μM) solution in the presence of different metal cations. [Fe³⁺] = 100 μM, [Na⁺, K⁺, Mg²⁺, Ca²⁺] = 1000 μM, and [other metal ions] = 200 μM.

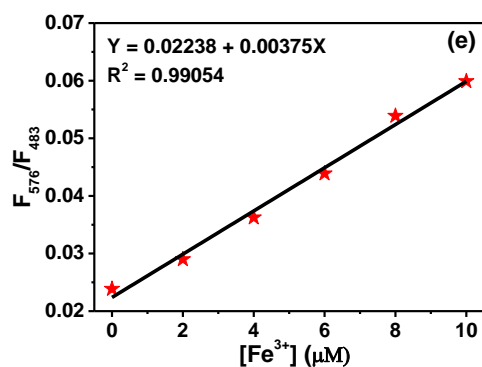


Figure S10 (a) Emission spectra of 10 μM **DRhFe** upon addition of Fe³⁺ (0-300 μM) in water (containing 1% DMSO). (b) Temporal profile of fluorescence intensity at 576 nm of **DRhFe** (10 μM) after being mixed with 150 μM Fe³⁺. $\lambda_{\text{ex}} = 543$ nm. (c) Job's plot of **DRhFe** in MeOH according to the emission intensity at 576 nm. The total concentration of **DRhFe** and Fe³⁺ was 20 μM. (d) Benesi–Hildebrand plot ($\lambda_{\text{abs}} = 561$ nm) of $1/(A - A_0)$ vs $1/[\text{Fe}^{3+}]$ based on a 1:1 association stoichiometry between **DRhFe** and Fe³⁺. (e) Plot of fluorescence intensity ratio of **DRhFe** as a function of Fe³⁺ concentration in the range of 0-10 μM.

S7. Fluorescent pH-dependence of DRhFe

The pH values of **DRhFe** solutions (10 μM, DMSO:H₂O = 1:99) were adjusted by KOH and HNO₃ solutions. The fluorescence spectra at different pH were collected in a 3 mL cuvette. After mixing with 10 eq. Fe³⁺, the fluorescence spectra were determined again. Then the pH-dependence was estimated according to the emission intensity ratio of F₅₇₆/F₄₈₃.

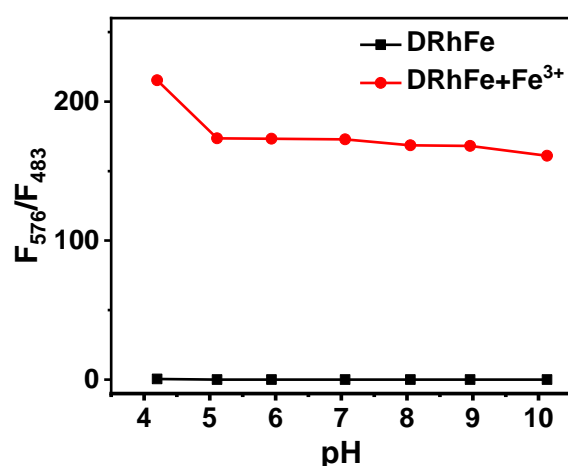


Figure S11 Emission ratio F₅₇₆/F₄₈₃ of **DRhFe** at different pH upon excitation at 405 nm and 543 nm in the absence or presence of 10 eq. Fe³⁺.

S8. Cytotoxicity determination of DRhFe

HeLa cells were cultured in Dulbecco's Modified Eagle Medium (DMEM, Invitrogen) media supplemented with 10% fetal bovine serum (FBS, heat-inactivated) and 100 U mL⁻¹ penicillin in 5% CO₂ atmosphere at 37°C. The cells were then seeded in the 24-well plates with 100,000 cells per well. Solutions of **DRhFe** (0, 5, 10, 20, and 40 µM) were added into the wells and incubated for 24 h at 37°C. [3-(4, 5-dimethylthiazol-2-yl)-2, 5-diphenyltetrazolium bromide] (MTT, 200 µL, 5 mg mL⁻¹ in PBS buffer, 1X) was then added into each well for further incubation (4 h). Next the medium was discarded and DMSO (200 µL) was added to dissolve the purple formazan. Then the absorbance at 570 nm of each well was recorded using a Varioskan Flash microplate reader (Thermo Scientific). The determination was carried out in triplicate to give the mean cell viability (%).

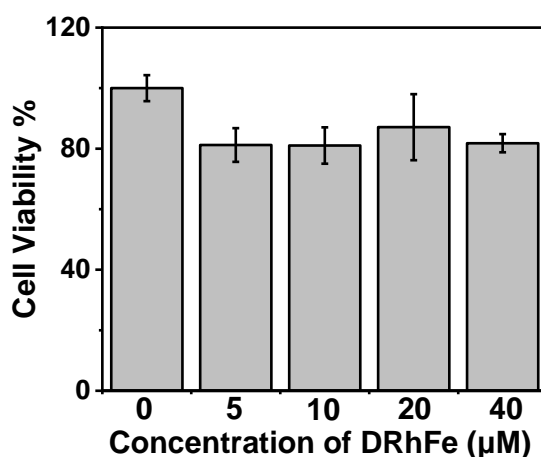


Figure S12 Cell viability of HeLa cells upon treatment (24 h at 37°C) with **DRhFe** at different concentration. Error bars represent standard deviations of 3 replicates.

S9. Ratiometric fluorescence imaging for exogenous labile Fe^{3+} in HeLa cells

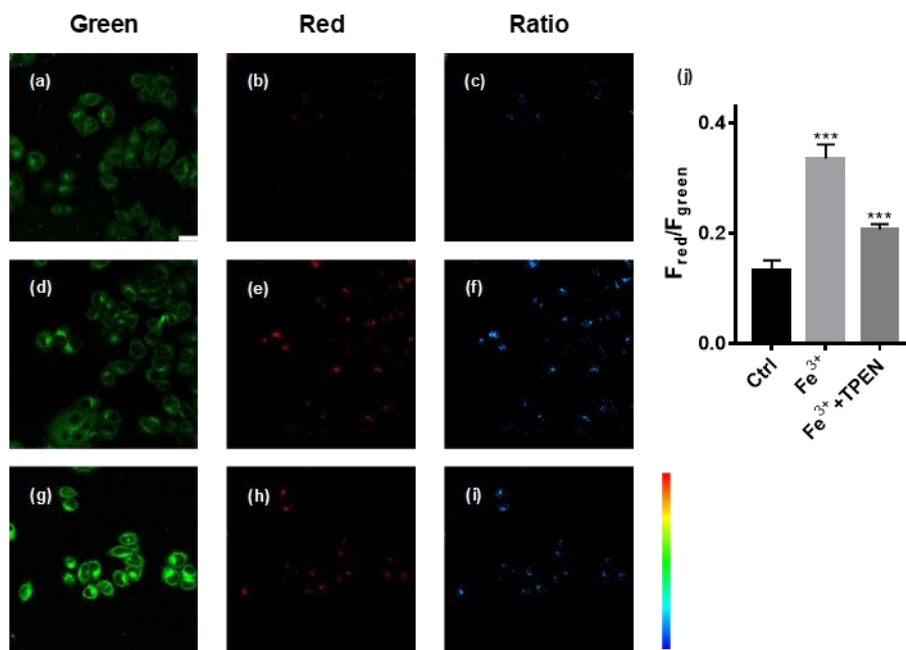


Figure S13. Confocal imaging of HeLa cells stained with **DRhFe** (10 μM , 30 min at 37°C) using a dual excitation/dual emission mode. (a-c) Cells were stained with only **DRhFe**; (d-f) **DRhFe**-stained cells preincubated with 20 μM Fe^{3+} for 8 h. (g-i) **DRhFe**-stained cells preincubated with 20 μM Fe^{3+} (8 h) and 20 μM TPEN (0.5 h) in sequence. (a), (d) and (g) Green channel images obtained with a bandpath of 440-500 nm upon excitation at 405 nm; (b), (e) and (h) red channel images obtained with a bandpath of 570-630 nm upon excitation at 561 nm; (c), (f) and (i) the corresponding ratiometric images; (j) average ratio of $F_{\text{red}}/F_{\text{green}}$ in (c), (f) and (i). Scale bars, 25 μm . Error bars represent standard deviations of 3 replicates. *** $P < 0.001$ versus Ctrl.

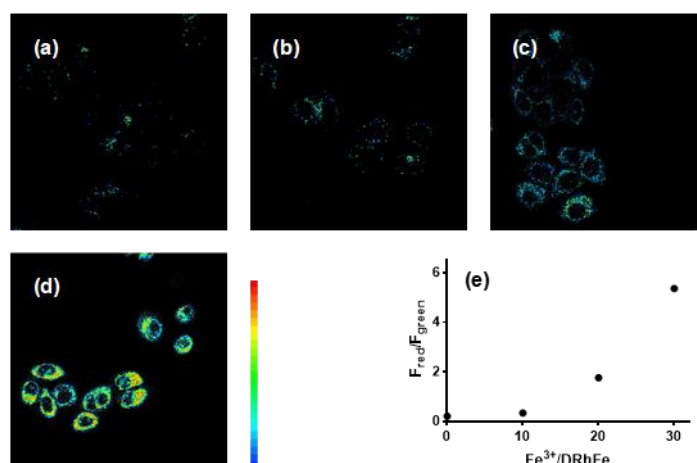


Figure S14. Confocal ratiometric images of HeLa cells stained by **DRhFe** (10 μM) upon increasing Fe^{3+} for 6 min. The imaging mode and parameters are the same as shown in Figure 3. (a) 0 Fe^{3+} , (b) 10 eq Fe^{3+} , (c) 20 eq Fe^{3+} , (d) 30 eq Fe^{3+} ; (e) average emission ratios of HeLa cells detected upon incubation at different Fe^{3+} .

S10. Ratiometric imaging of endogenous labile Fe^{3+} in cells undergoing ferroptosis

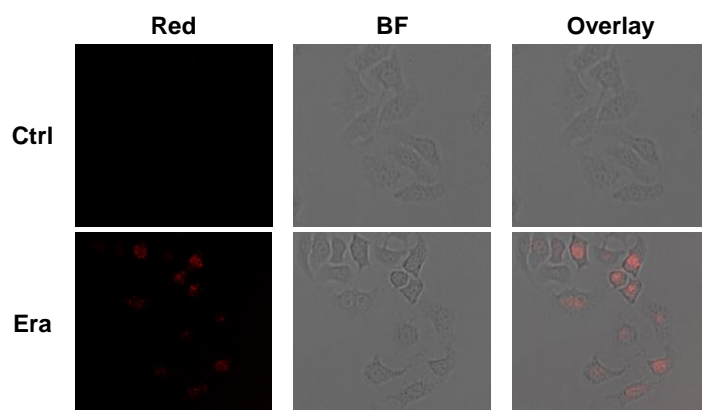


Figure S15. Confocal fluorescence imaging of MitoPeDPP-stained HeLa cells pretreated with 1 μM erastin for 8 h. The blank control without erastin incubation was also imaged for comparison.¹

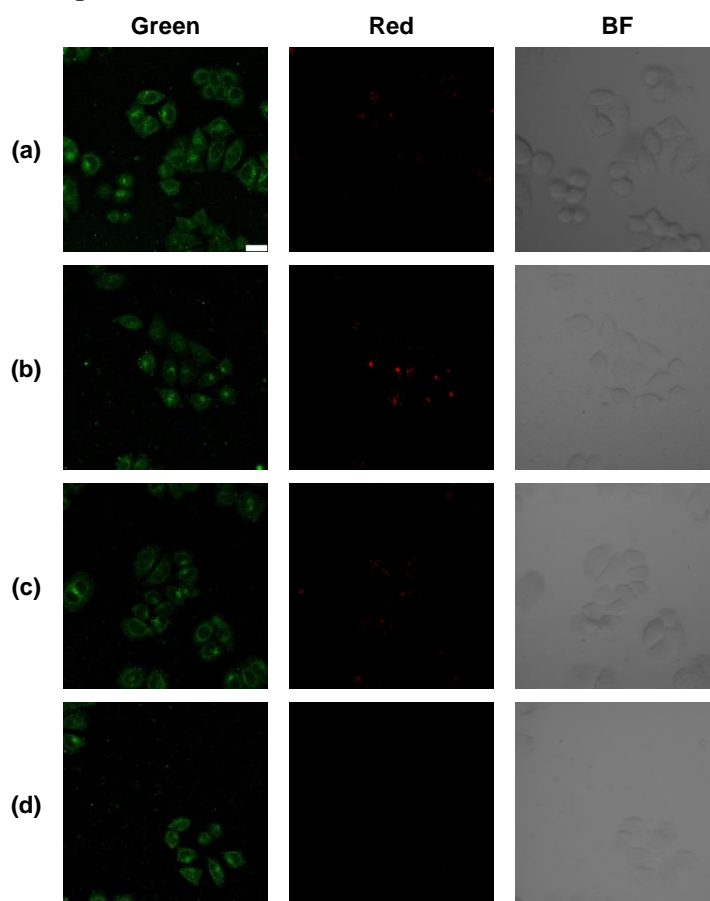


Figure S16. Confocal microscopy of living HeLa cells loaded with 10 μM **DRhFe**. Cells were pretreated with (a) control, (b) 1 μM Era, (c) 1 μM Era + 100 μM DFO, and (d) 1 μM Era + 1 μM Fer-1 for 8 hours. Green channel images obtained with a bandpath of 440-500 nm upon excitation at 405 nm, and red channel images obtained with a bandpath of 570-630 nm upon excitation at 561 nm. Scale bars, 25 μm .

S11. References:

- (1) Shioji, K.; Oyama, Y.; Okuma, K.; Nakagawa, H., Synthesis and properties of fluorescence probe for detection of peroxides in mitochondria. *Bioorg. Med. Chem. Lett.* **2010**, *20* (13), 3911-3915.